ELSEVIER

Journal of Magnetism and Magnetic Materials 231 (2001) 74–84

Journal of magnetism and magnetic materials

www.elsevier.com/locate/jmmm

A finite element analysis of the bending of crystalline plates due to anisotropic surface and film stress applied to magnetoelasticity

K. Dahmen[a], H. Ibach[a,*], D. Sander[b]

[a] *Institut für Grenzflächenforschung und Vakuumphysik, Forschungszentrum Jülich, 52425 Jülich, Germany*
[b] *Max-Planck-Institut für Mikrostrukturphysik, Weinberg 2, 06120 Halle, Germany*

Received 2 November 2000

Abstract

The bending of crystalline plates in response to a non-isotropic stress on one of the two surfaces is investigated with special attention to magnetoelastic effects. The crystalline plates are assumed to have cubic symmetry, expose either (1 0 0) or (1 1 1) surfaces, and be clamped along one edge. It is shown that the effect of clamping can be described by a dimensionless parameter, the "dimensionality" D, which in general depends on the length-to-width ratio of the sample, the Poisson ratio v, and the elastic anisotropy A. Using a finite element analysis we find that the dimensionality parameters for anisotropic and isotropic surface stresses are identical. The theory is applied to the bending caused by magnetoelastic stresses in deposited thin films. Expressions are derived to calculate the magnetoelastic coupling constants of films with cubic, tetragonal, or hexagonal symmetry from a measurement of the change of radius of curvature of the film–substrate composite upon an in-plane reorientation of the film magnetization.

PACS: 75.70; 75.70.Ak; 75.80

Keywords: Surface stress; Magnetoelastic coupling

1. Introduction

The cantilever bending technique is a well established method for the experimental determination of surface stress [1–7] as well as for magnetoelastic constants [8–13]. The basic idea of the method is to observe the bending of a thin sheet of material subject to an excess stress on one of the two surfaces. Rectangular crystalline samples clamped at one end are typically used. Because of the constraints on the bending imposed by the boundary condition of clamping, the bending becomes non-uniform and the surface stress cannot be calculated from the bending using the simple Stoney equation as discussed previously, see e.g. Ref. [14]. Neglecting the effect of the clamping can lead to a significant error of the order of 50% [15] in the surface stress or in the magnetoelastic constant. In a previous paper [15], we reported on finite element calculations on the

*Corresponding author. Tel.: +49-2461-614-561; fax: +49-2461-613-907.

E-mail address: h.ibach@fz-juelich.de (H. Ibach).

0304-8853/01/$ - see front matter
PII: S0304-8853(00)01392-5

bending of rectangular plates which are clamped along one edge. While we admitted cubic elastic anisotropy of the substrate, the surface stress was assumed to be isotropic. We showed that the effect of clamping can be expressed in terms of a single parameter, the "dimensionality" D, where the limiting cases of a pure one-dimensional or two-dimensional bending are characterized by $D = 1$ and 2, respectively. In this paper, we extend these calculations to the case of a non-isotropic stress load. Such non-isotropic loads are typical for the magnetoelastic stresses that are exploited to measure the magnetoelastic properties of thin magnetic films deposited on one side of a substrate crystal. We show that the effect of an anisotropic surface stress is described by the same dimensionality parameter as in the isotropic case, and a set of simple rules and equations for the determination of a magnetoelastic constant from the bending of the crystal plate is provided. Relations between the measured magnetoelastic constant of the deposited film and the magnetoelastic constants of bulk material are established by considering various common crystal structures for the thin films, including the contributions from different structural domains.

The paper is organized as follows. In order to make the paper self-contained, the next section provides a brief summary of the main results of the previous analysis [15] as well as the introduction to the notation. Section 3 addresses the bending of plates under the load of an anisotropic surface stress. It is shown how the components of the surface stress tensor can be obtained from the measurement of the curvature in two principal directions. Section 4 considers the special case of a film stress caused by a magnetoelastic coupling to an external field. It is shown that a magnetoelastic constant of the film can be determined directly from the measurement of the change in the curvature along one direction upon rotation of the magnetization, without using the frequently unknown elastic constants of the film. In Section 5 the effect of elastic interactions between different crystal domains in the film are studied and the relations between the film magnetoelastic constant and the components of the magnetoelastic coupling constants B_{ijkl} of bulk materials are established.

2. Bending of plates under the influence of an isotropic surface stress

In a typical cantilever bending experiment, a thin crystal with a rectangular shape is held in a fixed position by clamping along one edge. The notation used in the following is illustrated in Fig. 1. The crystalline plate with the thickness t has a length L parallel to the x_1-direction and a width W parallel to the x_2-direction (Fig. 1a). The bending is assumed to be measured in the center of the free end of the sample. Depending on the detection scheme for the experimental determination of the bending [1–13], either the displacement ζ, the slope ζ' or the curvature $\kappa = 1/R = (\zeta'(L_2) - \zeta'(L_1))/(L_2 - L_1)$ or a combination of the three is probed (Fig. 1b). In Ref. [15] we defined the displacement related "curvature κ_ζ"

$$\kappa_\zeta = \frac{2\zeta(L)}{L^2}, \tag{1}$$

the slope related "curvature $\kappa_{\zeta'}$"

$$\kappa_{\zeta'} = \frac{\zeta'(L)}{L}, \tag{2}$$

and the curvature $\kappa_{\zeta''}$

$$\kappa_{\zeta''} = \frac{\zeta'(L_2) - \zeta'(L_1)}{\Delta L} = \frac{\Delta\zeta'}{\Delta L} \approx \frac{\partial^2\zeta}{\partial x_1^2}. \tag{3}$$

In case of a uniform bending (constant curvature throughout the sample) the displacement and

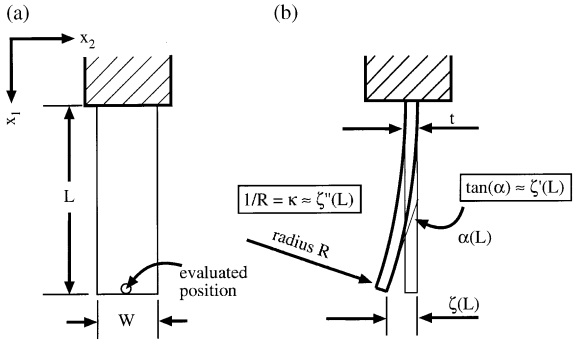

Fig. 1. Cantilever bending method: (a) A rectangular (crystalline) plate with the length L, the width W and the thickness t. (b) The induced change of the deflection ζ, or the change of the slope ζ' or the change of the curvature ζ'' can be measured in the center at the free end of the plate. The relations between the tilt angle α and the slope ζ' and between the local radius R and the curvature ζ'' are written down in the boxes.

slope related "curvatures" ($\kappa_\zeta, \kappa_{\zeta'}$) are identical to the true curvature $\kappa_{\zeta''}$. In the case considered here, which is a sample clamped on one end, they are not. The surface stress is determined from the measurement of either one of the "curvatures" with the help of elasticity theory. We restrict the considerations to cubic crystalline plates displaying (0 0 1)-surfaces with their x_1-direction oriented either along the [1 1 0]- or [1 0 0]-direction, and to cubic crystals with (1 1 1)-surfaces of arbitrary orientation. Hence, the surface has either C_{3v} or C_{4v} symmetry. We note in passing that the case of an HCP crystal with (0 0 0 1)-surfaces conforms with a cubic crystal with (1 1 1) surfaces. The elastic properties with respect to the crystal orientation are denoted by the Young modulus Y', the Poisson number ν' and the in-plane anisotropy parameter A'. These constants can be obtained from the elastic constants s_{11}, s_{12} and s_{44} of cubic crystals following established procedures [13,15,16]. The results are summarized in Table 1.

For an unsupported, free plate, a surface stress load with stress tensor components oriented parallel to the x_1- and x_2-direction is connected with the corresponding curvatures via the following two equations:

$$\kappa_1 = \frac{6}{t^2 Y'}\left[\tau_{11}^{(s)} - \nu'\tau_{22}^{(s)}\right], \tag{4}$$

$$\kappa_2 = \frac{6}{t^2 Y'}\left[\tau_{22}^{(s)} - \nu'\tau_{11}^{(s)}\right]. \tag{5}$$

Here, t represents the thickness of the plate. If the curvatures κ_1 and κ_2 in the x_1- and x_2-direction are measured, the principal components of the surface stress $\tau_{11}^{(s)}$ and $\tau_{22}^{(s)}$ can be calculated using Eqs. (4) and (5). This case is referred to as a "two-dimensional" bending. If the bending is constrained to one direction e.g., the x_1-direction, then the curvature deviates from the two-dimensional bending. For arbitrary $\tau_{22}^{(s)}$ the relation between the curvature κ_1 and the stress compo-nent $\tau_{11}^{(s)}$ is

$$\kappa_1 = \frac{6}{t^2 Y'}(1-\nu')(1+\nu')\tau_{11}^{(s)}. \tag{6}$$

The latter case is referred to as "one-dimensional" bending. In a realistic experiment, the sample is clamped along one edge (Fig. 1a). Then, the curvature is (mostly) between the one-dimensional limit Eq. (6) and the two-dimensional limit Eq. (4). In Ref. [15] we have shown that for an isotropic surface stress ($\tau_{11}^{(s)} = \tau_{22}^{(s)} = \tau^{(s)}$) the curvature κ_1 measured along the center line of the sample parallel to the x_1-direction (Fig. 1a) can be calculated using a generalized Stoney equation:

$$\kappa_1 = \frac{6}{t^2 Y'}(1-\nu')\left[1 + (2-D)\nu'\right]\tau^{(s)}. \tag{7}$$

All effects induced by the clamping of the sample are condensed into a single parameter, the "dimensionality D". The dimensionality D is 2 for a free plate. Eq. (7) is then equal to Eq. (4) for isotropic stress. Inserting $D=1$ makes Eq. (7) equal to Eq. (6). Hence, in the two limits, the dimensionality D as defined by Eq. (7) represents

Table 1
The relationship between the elastic compliance constants s_{ij} and the transformed elastic constants Y', ν' and A' for the crystal orientations which are elastically orthotropic ($s_{11}=s_{22}$) and have two axis of mirror symmetry. The constants Y, ν, and A are related to the (0 0 1)-plane oriented along the $\langle 1\,0\,0\rangle$ axis

Crystal plane / Crystal orientation	Y'	ν'	A'
$\frac{(0\,0\,1)}{\langle 1\,0\,0\rangle}$	$Y = \frac{1}{s_{11}}$	$\nu = -\frac{s_{12}}{s_{11}}$	A
$\frac{(0\,0\,1)}{\langle 1\,1\,0\rangle}$	$\frac{1}{s_{11} - 1/2\,S}$	$-\frac{s_{12} + 1/2\,S}{s_{11} - 1/2\,S}$	$\frac{1}{A}$
$\frac{\{1\,1\,1\}}{\text{All}}$	$\frac{1}{s_{11} - 1/2\,S}$	$-\frac{s_{12} + 1/6\,S}{s_{11} - 1/2\,S}$	1
$S = s_{11} - s_{12} - 1/2\,s_{44}$		$A = 2\frac{s_{11} - s_{12}}{s_{44}}$	

the true dimensionality of the problem. For all intermediate cases, the value of the dimensionality D depends on the method of the determination of the curvature (via ζ, ζ' or ζ''), the Poisson ratio ν', the in-plane anisotropy $A' = 2(s'_{11} - s'_{12})/s'_{44}$, the aspect ratio a = length/width of the sample, and on the position where the bending is measured. In Ref. [15] we calculated the full equilibrium shapes of thin plates under an isotropic surface stress load with the help of the finite element method. Here we briefly review the results of that calculation.

The dimensionality $D_{\zeta''}$ referring to the measurement of the local curvature $\kappa_{\zeta''}$, Eq. (3), is found to become independent of the elastic constants and has the value of roughly 2.0 for plates longer than about twice the width of the clamped edge. Hence, if the curvature is measured at the end of plates having an aspect ratio a larger than 2, the curvature is as for a free plate. A measurement of the curvature is, therefore, the most direct access route to experimental data on the surface stress and can be straightforwardly implemented by an optical deflection technique [17] which measures the change of slope $\Delta\zeta'$ of the sample between two points with a known separation $\Delta L'$, see Eq. (3).

The dimensionality $D_{\zeta'}$ measured with the change of the slope ζ' depends more significantly on the aspect ratio a and the elastic constants of the substrate. For $a \geqslant 2$ the dimensionality $D_{\zeta'}$ is well described by the approximate relation [15]

$$D_{\zeta'} = 2.0 - (0.29 + 0.10A')/a \quad \text{for } a \geqslant 2.0,$$
$$0.1 \leqslant \nu' \leqslant 0.6, \quad 0.25 \leqslant A' \leqslant 4.0. \tag{8}$$

This approximation gives a marginal error of less than 2.5% as compared to the numerical results, even in the worst case of large Poisson numbers ν' and high anisotropy parameters A', where the effect of clamping is most pronounced.

The dimensionality of samples determined via the displacement ζ always depends significantly on the aspect ratio a, the Poisson number ν' and the in-plane anisotropy A', even for long plates. The results of the calculations for D_ζ are presented in Fig. 2a and b, for the aspect ratios $a = 2$ and 5, respectively. Because of the dependence of the deflection on many parameters even for large aspect ratios the determination of the surface stress from the total deflection is more problematic than in other cases. This is somewhat unfortunate since the most sensitive methods for the determination of small bendings, the capacitance method [3,18] and the scanning tunneling microscope [4,5] measure the deflection.

3. Anisotropic surface stress

In the following, we generalize our earlier calculations for isotropic surface stresses and admit non-equal diagonal tensor components $\tau_{11}^{(s)}$, $\tau_{22}^{(s)}$ (in the reference frame of the principal axes along the x_1- and x_2-direction). For arbitrary components $\tau_{11}^{(s)}$ and $\tau_{22}^{(s)}$ the surface stress tensor can be decomposed into an isotropic tensor $\tau^{(s,+)}$ with equal diagonal components $\tau_{11}^{(s,+)} = \tau_{22}^{(s,+)}$ and an *antitropic* tensor $\tau^{(s,-)}$ with diagonal components which are the negative of each other $\tau_{11}^{(s,-)} = -\tau_{22}^{(s,-)}$

$$\begin{pmatrix} \tau_{11}^{(s)} & 0 \\ 0 & \tau_{22}^{(s)} \end{pmatrix} \equiv \frac{1}{2}(\tau_{11}^{(s)} + \tau_{22}^{(s)}) \begin{pmatrix} 1 & 0 \\ 0 & 1 \end{pmatrix} + \frac{1}{2}(\tau_{11}^{(s)} - \tau_{22}^{(s)}) \begin{pmatrix} 1 & 0 \\ 0 & -1 \end{pmatrix}. \tag{9}$$

The first part is $\tau^{(s,+)}$, the second $\tau^{(s,-)}$. The contribution of the isotropic part of the total surface stress $\tau^{(s,+)}$ to the curvature along the x_1-direction (measured via the displacement ζ, the slope ζ' or the true curvature ζ'') is according to Eq. (7):

$$\kappa_1^+ = \frac{6}{t^2 Y'}(1 - \nu')[1 + (2 - D^{(+)})\nu']\tau_{11}^{(s,+)}. \tag{10}$$

By considering the bending of an unclamped crystal with a free bending in two dimensions and the bending constrained to one dimension, one can derive a generalized Stoney relation also for the case of the antitropic part of surface stress $\tau^{(s,-)}$. The contribution to the curvature is then

$$\kappa_1^{(-)} = \frac{6}{t^2 Y'}(1 + \nu')\left[1 - (2 - D^{(-)})\nu'\right]\tau_{11}^{(s,-)}. \tag{11}$$

The isotropic and antitropic dimensionalities $D^{(+)}$ and $D^{(-)}$ depend on the measured type of curvature (κ_ζ, $\kappa_{\zeta'}$ or $\kappa_{\zeta''}$, Eqs. (1–3)), as in the

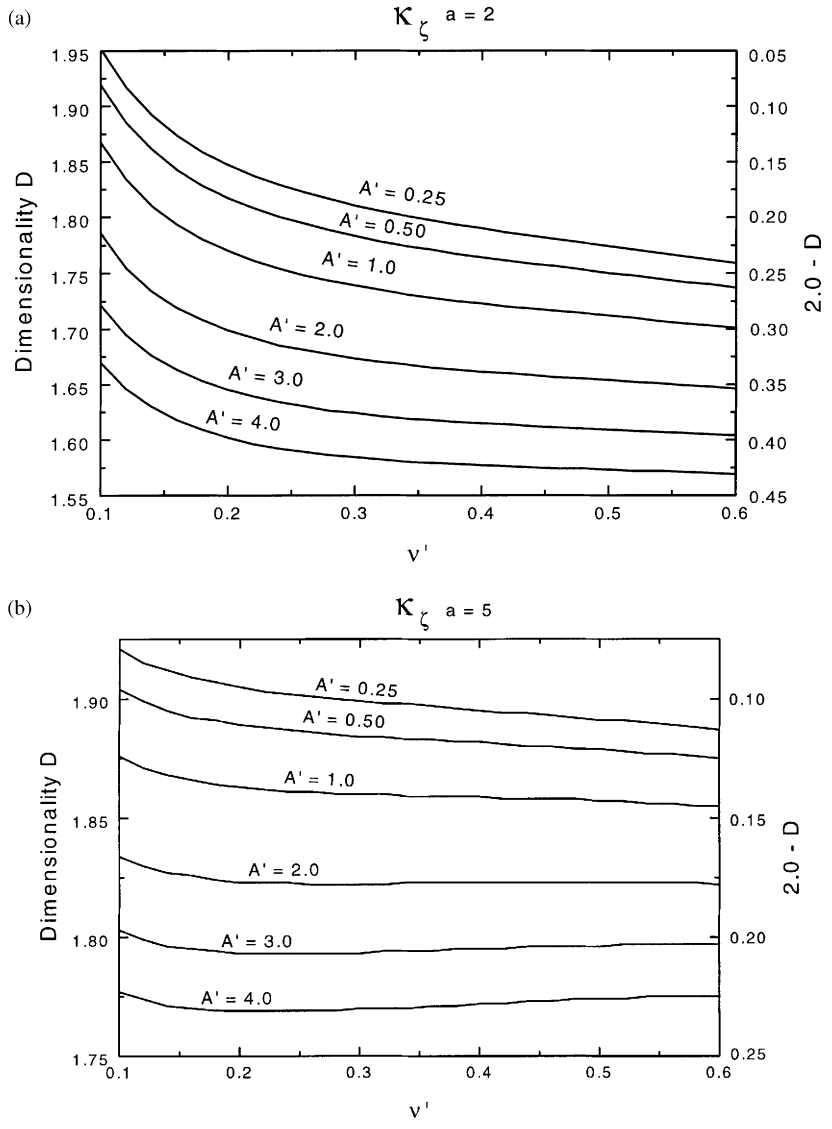

Fig. 2. Dimensionality D for κ_ζ referring to the deflection of an elastically anisotropic plate clamped along one edge and loaded with an isotropic or anisotropic surface stress on one surface as a function of the Poisson number ν' and the anisotropy A' for the aspect ratio (a) $a=2$ and (b) $a=5$.

isotropic case. Because of the linearity of the bending for small loads, the total bending arising from an arbitrary stress load is the sum of the bending caused by the isotropic and antitropic parts of the surface stress tensor. Hence, by decomposing the surface stress into an isotropic and antitropic part, one can calculate the bending for general anisotropic surface stresses also. All geometric factors are contained in the dimensionalities $D^{(+)}$ and $D^{(-)}$. With the abbreviation

$$F^{(+/-)} = \frac{6}{t^2 Y'}(1 \mp \nu')[1 \pm (2 - D^{(+/-)})\nu'], \qquad (12)$$

the total curvature along the x_1-direction is

$$\kappa_1 = \kappa_1^{(+)} + \kappa_1^{(-)} = F^{(+)}\,\tau_{11}^{(s,+)} + F^{(-)}\,\tau_{11}^{(s,-)} = \frac{1}{2}(F^{(+)} + F^{(-)})\tau_{11}^{(s)} + \frac{1}{2}(F^{(+)} - F^{(-)})\tau_{22}^{(s)}. \quad (13)$$

In Ref. [15] the isotropic dimensionality $D^{(+)}$ was calculated. We have now extended our finite element analysis to the case of an antitropic stress load. For all aspect ratios a, Poisson ratios ν' and elastic anisotropies A' we find

$$D^{(-)} = D^{(+)}. \quad (14)$$

This relation can presumably be proven analytically from general symmetry principles; we were, however, unable to do so. From the practical standpoint, Eq. (12) is very convenient since the values for $D^{(+)}$ calculated in Ref. [15] (see also Eq. (8) and Fig. 2) transfer directly to the antitropic case. We note that the stress considered in the work of Watts et al. [20] is of antitropic nature. Their calculations for κ_ζ, $\nu' = 0.22$, $A' = 1$ and the aspect ratios a ranging from 0.0625 to 16 match our results exactly.

In most cases one is interested in the determination of the surface stress from a measured bending of the substrate. For the determination of the two independent components of an anisotropic surface stress tensor, one needs to measure in addition the curvature along the x_2-direction. In an analogy to Eq. (13), one can write down the equivalent equation for the curvature κ_2. The transverse dimensionality entering the equation for κ_2 which differs from the longitudinal dimensionality as defined above can again be calculated using finite element methods. For the surfaces considered here having either C_{3v} or C_{4v}-symmetry, the macroscopic surface stress as measured by the cantilever bending method is necessarily isotropic. This holds even if the local symmetry is lower due to the structure of the surface or the thin deposited film. In that case, an equal number of domains of different orientation exist to make the overall surface stress isotropic. A possible anisotropy of the actual bending, as reflected in different numbers for the longitudinal and transverse dimensionality is only an effect of the clamping. Hence, if the experimental method permits an independent measurement of the two curvatures, one may compare these measurements for an estimate on the residual effect of the clamping.

4. Magnetoelastic coupling

The cantilever bending method has a long tradition in the experimental determination of magnetoelastic coupling constants of thin films [8,9,19] and the discussion of the curvature analysis has attracted a series of publications [20–27]. While the importance of the clamping condition on the bending was realized in earlier papers, no detailed analysis has been presented so far, except for the numerical calculation of Watts et al. for a special set of elastic constants of the substrate [28]. Other previous treatments considered either merely a two-dimensional bending of a free plate or a one-dimensional bending. These extremes correspond to large and small length-to-width ratios of the film–substrate composite, respectively. With the curvature analysis presented in Section 3, magnetoelastic data of the film can now be extracted from measurements on crystalline samples with a wide range of aspect ratios, provided that their surfaces have C_{3v} or C_{4v} symmetry. By making use of the results above, we show that the effective magnetoelastic coupling constant B_{eff} is obtained by measuring the change of a single curvature upon re-orientation of the magnetization. In several recent papers, the magnetoelastic effects of films with various orientations and with different domain structure on the surface were considered and the effect of film strain on the modified magnetoelastic properties has been investigated [12,17,29–31]. Our analysis, therefore, includes the consideration of films with crystal structures which differ from the substrate and also films which consist of differently oriented domains. The discussion is restricted to the case of thin deposited films so that the effect of the (bulk) magnetoelastic stress tensor τ_f in the magnetic film on the bending of the substrate plate can be treated as a surface stress $\tau^{(s)} = t_f\tau_f$, with $t_f < t$ the thickness of the film.

We consider the difference in the bending of a plate for the magnetization either oriented along the x_1- or the x_2-direction. The bending itself can

be measured as $\kappa_1 = \kappa_{1\zeta}$, $\kappa_1 = \kappa_{1\zeta'}$, or as $\kappa_1 = \kappa_{1\zeta''}$ at the end of the plate (Fig. 1a). Because of the symmetry of the substrate, the components of the surface stress tensor (averaged over structural domains) obey the relations

$$\begin{aligned}\tau_{11}^{(s)}(M\|x_1) &= \tau_{22}^{(s)}(M\|x_2),\\ \tau_{11}^{(s)}(M\|x_2) &= \tau_{22}^{(s)}(M\|x_1),\end{aligned} \tag{15}$$

where $M\|x_1$ and $M\|x_2$ denote a film magnetization along the sample length and along the sample width, respectively. It is assumed that for each magnetization state a saturated, single domain magnetization state of the whole film is obtained, as should be verified experimentally, e.g. by magneto-optical Kerr effect measurements [32].

With Eq. (15) inserted into Eq. (13) one obtains for the change in κ_1 upon a rotation of the magnetization by 90°

$$\begin{aligned}\Delta\kappa_1 &\equiv \kappa_1(M\|x_1) - \kappa_1(M\|x_2)\\ &= F^{(-)}\left(\tau_{11}^{(s)}(M\|x_1) - \tau_{22}^{(s)}(M\|x_1)\right)\end{aligned} \tag{16}$$

or alternatively

$$\begin{aligned}\Delta\kappa_1 &\equiv \kappa_1(M\|x_1) - \kappa_1(M\|x_2)\\ &= F^{(-)}\left(\tau_{11}^{(s)}(M\|x_1) - \tau_{11}^{(s)}(M\|x_2)\right)\end{aligned} \tag{17}$$

with $F^{(-)} = (6/t^2\,Y')\,(1+\nu')[1-(2-D^{(-)})\nu']$ from Eq. (12).

Using these remarkably simple equations, the change in the curvature can be calculated from the magnetoelastic stresses. The stresses in turn are related to the magnetoelastic coupling constants. Depending on the crystal structure of the magnetic film and the orientation of the crystal domains with respect to the substrate, a particular coupling constant of the magnetic film or combinations thereof are determined by measuring the change of curvature $\Delta\kappa_1$ upon an in-plane reorientation of the magnetization. The general form of the magnetoelastic energy density $f_{\rm me}$ can be written as

$$f_{\rm me} = \sum B_{ijkl}\varepsilon'_{ij}\alpha'_k\alpha'_l + \cdots, \tag{18}$$

where B_{ijkl} is a tensor of the magnetoelastic coupling constants, ε'_{ij} the strain tensor, and α'_k are the cosines of the orientation of the magnetization with respect to the crystal axes in the crystal structure of the film. Higher order contributions, indicated by dots, are neglected for clarity. Note however, that recent experimental and theoretical work indicate a significant contribution of second order strain terms to the magnetoelastic energy density in Eq. (18), see e.g. Refs. [30,33,34]. We introduce the magnetoelastic tensor B_{ijkl} in analogy to the magnetostrictive tensor as defined by Mason [35,36]. In contrast to bulk ferromagnets, the use of a magnetoelastic tensor is more appropriate for thin films, as magnetization processes induce magnetoelastic stresses that are given by the strain derivative of Eq. (18). A direct calculation of magnetostrictive strain is only possible for bulk samples, whereas for supported films the resulting strain depends on the rigidity of the substrate, as will be shown below. The magnetoelastic tensor B_{ijkl} has a reduced symmetry as compared to the elasticity tensor c_{ijkl}. In particular, the off-diagonal elements B_{1133} and B_{3311} for tetragonal or hexagonal cystals need not be equal. For a tetragonal crystal (the direction of the c-axis denoted by the index 3), the non-vanishing terms in the sum (18) are

$$\begin{aligned}f_{\rm me} = {} & B_{1111}(\varepsilon'_{11}\,\alpha_1'^2 + \varepsilon'_{22}\,\alpha_2'^2) + B_{3333}\,\varepsilon'_{33}\,\alpha_3'^2\\ & + B_{1122}(\varepsilon'_{11}\,\alpha_2'^2 + \varepsilon'_{22}\,\alpha_1'^2)\\ & + B_{1133}(\varepsilon'_{11} + \varepsilon'_{22})\,\alpha_3'^2\\ & + B_{3311}\,\varepsilon'_{33}(\alpha_1'^2 + \alpha_2'^2)\\ & + 4B_{1313}(\varepsilon'_{23}\,\alpha'_2\,\alpha'_3 + \varepsilon'_{13}\,\alpha'_1\,\alpha'_3)\\ & + 4B_{1212}\,\varepsilon'_{12}\,\alpha'_1\,\alpha'_2.\end{aligned} \tag{19}$$

The seven independent magnetoelastic constants B_{ijkl} of the tetragonal system reduce further for higher crystalline symmetry. The hexagonal symmetry requires a constant magnetoelastic contribution for a rotation within the basal plane by 60° and this leads to the relation

$$B_{1212} = \frac{1}{2}(B_{1111} - B_{1122}). \tag{20}$$

Here, we are only interested in the orientation dependence of the magnetoelastic energy, and the number of independent constants reduces further because of the normalization condition $\sum_i \alpha_i'^2 = 1$. Omitting terms that are independent of the magnetization direction α_i, Eq. (19) reduces for

a hexagonal crystal to

$$f_{\rm me} = B_1(\varepsilon'_{11}\,\alpha'^2_1 + 2\varepsilon'_{12}\,\alpha'_1\,\alpha'_2 + \varepsilon'_{22}\,\alpha'^2_2) + B_2\,\varepsilon'_{33}(1-\alpha'^2_3) + B_3(\varepsilon'_{11}+\varepsilon'_{22})(1-\alpha'^2_3) + B_4(2\varepsilon'_{23}\,\alpha'_2\,\alpha'_3 + 2\varepsilon'_{13}\,\alpha'_1\,\alpha'_3), \quad (21)$$

where

$$B_1 = B_{1111} - B_{1122}, \quad B_2 = B_{3311} - B_{3333}, \quad B_3 = B_{1122} - B_{1133}, \quad B_4 = 2\,B_{1313}. \quad (22)$$

The constants B_i are the four independent magnetoelastic constants in the standard notation [13,30]. For a cubic crystal the orientation dependence of the magnetoelastic energy can be written as

$$f_{\rm me} = B_1(\varepsilon'_{11}\,\alpha'^2_1 + \varepsilon'_{22}\,\alpha'^2_2 + \varepsilon'_{33}\,\alpha'^2_3) + B_2(2\,\varepsilon'_{23}\,\alpha'_2\,\alpha'_3 + 2\,\varepsilon'_{13}\,\alpha'_1\,\alpha'_3 + 2\,\varepsilon'_{12}\,\alpha'_1\,\alpha'_2) \quad (23)$$

with

$$B_1 = B_{1111} - B_{1122} \quad \text{and} \quad B_2 = 2B_{2323}. \quad (24)$$

The components of the magnetic surface stress tensor $\tau^{(s)}_{ij}$ for a particular orientation of the magnetization $\hat{M}$ in the magnetic film having the thickness $t_{\rm f}$ are given by the derivative

$$\tau^{(s)}_{ij} = t_{\rm f}\,\tau_{ij} = t_{\rm f}\,\frac{\partial f_{\rm me}(\hat{\rm M})}{\partial \varepsilon_{ij}}. \quad (25)$$

Here, $\partial/\partial\varepsilon_{ij}$ are the strain derivatives with respect to the x_1- and x_2-axis of the substrate plate. For a general orientation of the crystal axes in the magnetic film, the energy $f_{\rm me}(\varepsilon'_{ij}, \alpha'_k)$ has to be expressed in terms of the strains and angles in the substrate crystal coordinate system. By combining Eq. (25) with Eqs. (16) or (17), the variation of the curvature upon a rotation of the magnetization by 90° can be related to certain components of the magnetoelastic tensor B_{ijkl}. The analysis does not require the knowledge of the elastic constants of the film. The elastic constants of the film enter only if the bending effect is expressed in terms of the magnetostriction constants λ of the film. Since the elastic constants of the film are not well known, in particular when the film is only a few monolayers thick, the analysis proposed here involves less uncertainties, as already discussed by Sander [13].

5. Cantilever bending and magnetoelastic constants of deposited films

This section addresses the question which magnetoelastic coupling constant of a magnetic thin film is measured in a cantilever bending experiment when the magnetization is rotated by 90°. The answer to this question depends on the crystal structure of the deposited film and the orientation of the crystal axes with respect to the underlying substrate. Several special cases have already been discussed in Ref. [17]. Here, a systematic analysis is provided. The effective magnetoelastic coupling constant measured by the cantilever method integrates over the thickness of the magnetic film and we focus on magnetoelastic stresses which are proportional to the film thickness. Thus, an effective magnetoelastic coupling constant is measured and subsequent experiments are mandatory to explore the physical origin of the often observed deviation of the magnetoelastic coupling in ferromagnetic monolayers from the respective bulk values [12,30,31,37,38].

In the first step, we comment on the effect of a domain structure in the deposited films. Domains of different orientation are often encountered in thin film epitaxy. It is thus important to understand how the magnetic stresses in the individual domains add up to the macroscopic surface stress measured by the cantilever method. The simplest approach would be to assume that the total magnetoelastic energy is the sum over the magnetoelastic energies of the domains. This neglects interaction terms arising from the coupling of strain fields extending into the bulk of the film and the substrate, and it is therefore necessary to estimate the magnitude of the interaction energy. The problem of the elastic coupling between domains of different orientation has been discussed frequently in the context of the stress-strain driven self-assembly of nanostructures. A simple analytical solution for the interaction energy exists for the case of stress domains in the form of stripes of infinite length. It is straightforward to see that for this geometry the interaction is stronger than for two-dimensional domains, since for the stripes the strain fields extend more deeply into the bulk. The analytical solution available for the

interaction energy of striped stress domains [39] can therefore serve to estimate an upper limit for the interaction. For the stripe geometry, the strain derivative of the interaction energy leads to a stress perpendicular to the stripes. The ratio of this stress $\tau_{\rm int}$ to the mean magnetoelastic stress τ in the domain is

$$\frac{\tau_{\rm int}}{\tau} = \frac{3}{8\pi}\frac{(\tau_{\|}-\tau_{\perp})^2}{\bar{\tau}^2}\frac{\bar{\tau}\,t_{\rm f}}{\ell\,\mu}\left(\ln(\ell/\pi a_{\rm d})-1\right). \tag{26}$$

Here $\tau_{\|}$, $\tau_{\perp}$, and $\bar{\tau}$ are the magnetic stresses parallel and perpendicular to the stripes for a given orientation of the magnetization and the mean magnetoelastic stress, respectively. The width of the stripes and the width of the domain walls are denoted as ℓ and $a_{\rm d}$, respectively, and $\mu = (c_{11} - c_{12} + 4c_{44})/6$ is an elastic constant of the substrate if $\ell \gg t_{\rm f}$. Since the magnitude of the magnetoelastic stresses are given by the magnetoelastic coupling constants B_i, which are of the order of several MPa and are thus very small compared to the elastic constants of roughly 100 GPa, the ratio $\tau_{\rm int}/\tau$ is also small, even for small domain widths ℓ and large film thickness $t_{\rm f}$. For two-dimensional domain configurations the interaction term is even smaller for reasons discussed above. The magnetic stresses and the bending caused by magnetoelastic effects for films with different domains can therefore be calculated from the magnetic energy taken as the sum over the various domains. With Eqs. (16), (17), and (20) the change in the curvature along the x_1-direction upon rotating the magnetization from the x_1-direction into the x_2-direction is

$$\Delta\kappa_1 = F^{(-)}\,t_{\rm f}\,B_{\rm eff}, \tag{27}$$

where $B_{\rm eff}$ represents the average effective magnetoelastic coupling constant of the film. This magnetoelastic constant is an unequivocal experimental result and as such not affected by possibly debatable assumptions and interpretations.

In ultra-thin films the crystal symmetry is reduced due to the interaction with the substrate. A heteroepitaxial film of a cubic material on the (1 0 0) surface of a cubic substrate, e.g., is laterally strained because of the mismatch of the lattice constants of the two materials. The lateral strain causes a tetragonal distortion of the film, so that the film structure becomes tetragonal. The magnetoelastic constant of that film may be quite

Table 2
Effective magnetoelastic coupling constants $B_{\rm eff}$ measured in cantilever bending experiment on a substrate with a C_{3v} or C_{4v} surface symmetry for various common crystal structures of epitaxial magnetic films. The quoted magnetoelastic coupling constants B_{ijkl} or combinations thereof are measured from a change of radius of curvature $\Delta\kappa$ during an in-plane reorientation of the magnetization, see Eqs. (27) and (17)

Case no.	Film structure	$B_{\rm eff}$
1	Cubic or tetragonal with axes along x_1 and x_2	$B_{1111}-B_{1122}$ ($=B_1$ for a cubic crystal)
2	Hexagonal, c-axis perpendicular to surface	$B_{1111}-B_{1122}=2B_{1212}=B_1$
3	Cubic or tetragonal rotated by 45° with respect to x_1, x_2	$2B_{1212}$ ($=B_2$ for a cubic crystal)
4	Tetragonal and hexagonal with c-axis in plane, or orthorhombic, 2 domains parallel x_1, x_2	$\frac{1}{2}(B_{3333}+B_{1111}-B_{1133}-B_{3311})$
5	Tetragonal and hexagonal with c-axis in plane, or orthorhombic, 2 domain rotated by 45° with respect to x_1, x_2	$2B_{1313}$ ($=B_4$ for a hexagonal crystal)
6	Cubic or tetragonal with c-axis perpendicular to surface, 3 domains rotated by 120°	$\frac{1}{2}(B_{1111}-B_{1122})+B_{1212}$
7	Tetragonal and hexagonal with c-axis in plane, or orthorhombic, 3 domains rotated by 120°	$\frac{1}{4}(B_{1111}+B_{3333}-B_{1133}-B_{3311})+B_{1313}$

different from the magnetoelastic constant of the undistorted cubic phase. Quite frequently, the lattice mismatch and the interaction with the substrate stabilizes phases which otherwise would not be stable at all, or would not be stable at the same temperature. In order to understand the magnetoelastic effect of the film, it is useful to be able to relate the measured magnetoelastic constant of the film, as measured by the cantilever method, to the magnetoelastic constants of the corresponding bulk material. To establish these relations, the magnetic energy of the particular crystal domains in the thin film (Eqs. (19) and (21)) has to be expressed in terms of the substrate coordinates. The magnetic stresses are then calculated according to Eq. (25). The results for various common crystal structure of the film are listed in Table 2. Cases 1–5 are relevant for substrate surfaces with C_{4v}-symmetry and cases 6 and 7 for substrate surfaces with C_{3v}-symmetry. The single-index constants B_i notation (Eqs. (22) and (24)) is also given where possible. Since only magnetoelastic constant with indices referring to the in-plane crystallographic axes appears, the results for the hexagonal and tetragonal crystal with the c-axis oriented in the surface plane also apply to orthorhombic films (cases 4,5, and 7). For the orthorhombic lattice the indices 1 and 3 refer to the two crystal axes within the plane of the film. Some of the cases in Table 2 have already been discussed in Refs. [13,17]. As seen from Table 2, the cantilever bending experiment determines a very special combination of the bulk magnetoelastic constants of the film which depends on the structure and orientation of the film. A complete characterization of the magnetoelastic properties is, therefore, not possible with a single curvature measurement.

Acknowledgements

Partial support of this work by the 'Fond der Chemischen Industrie is gratefully acknowledged. We thank Dr. T. Gutjahr-Löser for the fruitful discussions concerning the nature of the magnetoelastic coupling in thin films.

References

[1] A.J. Schell-Sorokin, R.M. Tromp, Phys. Rev. Lett. 64 (1990) 1039.
[2] R.A. Martínez, W.M. Augustyniak, J.A. Golovchenko, Phys. Rev. Lett. 64 (1990) 1035.
[3] D. Sander, H. Ibach, Phys. Rev. B 43 (1991) 4263.
[4] C.E. Bach, M. Giesen, H. Ibach, T.L. Einstein, Phys. Rev. Lett. 78 (1997) 4225.
[5] H. Ibach, C.E. Bach, M. Giesen, A. Grossmann, Surf. Sci. 375 (1997) 107.
[6] W. Haiss, J.K. Sass, J. Electroanal. Chem. 386 (1995) 267.
[7] W. Haiss, R.J. Nichols, J.K. Sass, J. Electroanal. Chem. 452 (1998) 199.
[8] E. Klokholm, IEEE Trans. Magn. MAG-12 (1976) 819.
[9] A.C. Tam, H. Schroeder, J. Appl. Phys. 64 (1988) 5422.
[10] M. Weber, R. Koch, K.H. Rieder, Phys. Rev. Lett. 73 (1994) 1166.
[11] J. Betz, E.d.T.d. Lacheisserie, L.T. Baczewski, Appl. Phys. Lett. 68 (1996) 132.
[12] R. Koch, J.J. Schulz, K.H. Rieder, Europhys. Lett. (1999) 554.
[13] D. Sander, Rep. Prog. Phys. 62 (1999) 809.
[14] H. Ibach, Surf. Sci. Rep. 29 (1997) 193.
[15] K. Dahmen, S. Lehwald, H. Ibach, Surf. Sci. 446 (2000) 161.
[16] W.A. Brantley, J. Appl. Phys. 44 (1973) 534.
[17] T. Gutjahr-Löser, Magnetoelastische Kopplung in oligatomaren Filmen, Verlag für Wissenschaft und Forschung, Berlin, 1999.
[18] R. Koch, M. Weber, E. Henze, K.H. Rieder, Surf. Sci. 331–333 (1995) 1398.
[19] A.C. Tam, H. Schroeder, IEEE Trans. Magn. 25 (1989) 2629.
[20] E.v.d. Ried, J. Appl. Phys. 76 (1994) 584.
[21] E.d.T.d. Lacheisserie, J.C. Peuzin, J. Magn. Magn. Mater. 136 (1994) 189.
[22] E.d.T.d. Lacheisserie, Phys. Rev. B 51 (1995) 15925.
[23] P.M. Marcus, Phys. Rev. B 53 (1996) 2481.
[24] P.M. Marcus, Phys. Rev. B 54 (1996) 3662.
[25] P.M. Marcus, J. Magn. Magn. Mater. 168 (1997) 18.
[26] E. Klokholm, C.V. Jahnes, J. Magn. Magn. Mater. 152 (1996) 226.
[27] E.d.T.d. Lacheisserie, J.C. Peuzin, J. Magn. Magn. Mater. 152 (1996) 231.
[28] R. Watts, M.R.J. Gibbs, W.J. Karl, H. Szymczak, Appl. Phys. Lett. 70 (1997) 2607.
[29] D. Sander, A. Enders, J. Kirschner, J. Magn. Magn. Mater. 198–199 (1999) 519.
[30] T. Gutjahr-Löser, D. Sander, J. Kirschner, J. Magn. Magn. Mater. 220 (2000) L1.
[31] T. Gutjahr-Löser, D. Sander, J. Kirschner, J. Appl. Phys. 87 (2000) 5920.
[32] D. Sander, R. Skomski, A. Enders, C. Schmidthals, D. Reuter, J. Kirschner, J. Phys. D 31 (1998) 663.

[33] M. Fähnle, M. Komelj, J. Magn. Magn. Mater. 220 (2000) L13.
[34] M. Komelj, M. Fähnle, J. Magn. Magn. Mater. 220 (2000) L8.
[35] W.P. Mason, Phys. Rev. 82 (1951) 715.
[36] W.P. Mason, Phys. Rev. 96 (1954) 302.
[37] A. Enders, D. Sander, J. Kirschner, J. Appl. Phys. 85 (1999) 5279.
[38] R. Koch, M. Weber, K.H. Rieder, J. Magn. Magn. Mater. 159 (1996) L11.
[39] O.L. Alerhand, D. Vanderbilt, R.D. Meade, J.D. Joannopoulos, Phys. Rev. Lett. 61 (1988) 1973.